CELLULOSE ACETATE/COPPER (II) OXIDE NANOCOMPOSITE FOR SELECTIVE DETECTION AND EXTRACTION OF LEAD (II) IONS

KHALID ALAMRY,[*] SHER KHAN,[*,**] ELHAM BIFARI[*] and ABDULLAH ASIRI[*,**]

[*]*Chemistry Department, Faculty of Science, King Abdulaziz University,*
P. O. Box 80203, Jeddah 21589, Saudi Arabia
[**]*Center of Excellence for Advanced Materials Research (CEAMR), King Abdulaziz University,*
P. O. Box 80203, Jeddah 21589, Saudi Arabia
✉ *Corresponding author: K. A. Alamry, kaalamri@kau.edu.sa*

Nanocomposites (NCs) based on cellulose acetate (CA) were prepared by dispersing copper (II) oxide (CuO) nanofillers in the cellulose acetate matrix. Nanocomposites were structurally examined by different spectroscopic techniques. The CA/CuO NCs were immobilized on a silver electrode (AgE) to investigate its chemical sensing behavior toward lead ions by I-V (current *vs.* voltage) technique. The calibration curve showed good electrical response toward Pb^{+2} with linearity up to 100 µM. The linear range exhibited good sensitivity (213.43 $\mu A.cm^{-2}.mM^{-1}$). The electrical performance showed an optimum response at pH 6 and good selectivity toward Pb^{+2}, compared to the interference of other metal ions. Further, the selectivity of NCs toward different metal ions, including Zn^{2+}, Ni^{2+}, Pb^{2+}, Mn^{2+}, Sr^{3+}, Al^{3+}, Fe^{3+} and Ce^{3+}, was investigated by inductively coupled plasma optical emission spectroscopy. CA/CuO (3% w/w) displayed higher uptake capacity for Pb^{2+} with K_d of 344170 mL/g. These data revealed that CA/CuO NCs exhibit high sensitivity and selectivity toward detection and extraction of lead ions and could be used for the efficient removal of Pb^2.

Keywords: cellulose acetate, CuO, nanocomposite, sensor, lead ion, detection, extraction, water treatment

INTRODUCTION

Environmental contamination with lead (Pb) has become a growing issue because of the serious toxic effects of Pb on human health. Several reports claim that exposure to lead, even at trace levels, may cause some serious damaging, such as irritability, muscle paralysis, nerve disorders and memory loss. Therefore, the identification of lead at trace levels in the environment and its extraction have become a topic of major interest.[1-6]

Several techniques have been successfully used for determining trace heavy metals.[7-10] However, due to the simplicity, low cost, fast response and high sensitivity and specificity, the electrochemical techniques have been established as promising methods for the determination of heavy metal ions. Polymer modified electrodes have been recently used in electrochemical applications since the characteristic properties of the polymer used, such as its catalytic, permeability, preconcentration and transport properties, helped to further promote the performance of the electrochemical analysis.[11-13] Modified electrodes in the electrochemical analysis of trace heavy metals can bring out several advantages, such as an improvement in the sensitivity and selectivity of trace analytes, as well as reduction of contaminants and competing ligands.[5,14] Thus, to further improve the properties of these polymers, and subsequently boost up electrochemical analysis, several advances have been made in nanotechnology by the development of polymer nanocomposites.[15,16] Among the nanofillers used, metal oxide nanomaterials have been considered as great candidates in chemical sensing and biosensing due to their thermal stability, chemical inertness with chemicals and biomolecules, and low temperature operation,[17] in addition to the possibility of manipulating their surfaces to make them suitable enough for the proposed application.[18]

The field of material science and nanotechnology has motivated scientists all over the world to advance materials with innovative

properties that cannot be encountered in conventional materials.[19-22] The development of nanocomposites has increased markedly in recent years due to the great potential associated with this new generation of extraordinary materials.[23-27] Nanocomposites research embraces a wide spectrum of applications, such as data storage, electronics and computing, communications, transportation, health and medicine, aerospace and sports materials, energy, environmental, and national defence applications.[28-31]

Cellulose acetate (CA) is an important bio-based polymer that has been used in a broad range of applications.[32-34] Even though, CA has played a significant role in various applications, the incorporation of various nanofillers, such as CNT, clays, metal oxides, nanoparticles *etc.*, can lead to developing a CA polymer with a suitable property profile for countless applications and utilization possibilities.[35-37] According to literature, several studies have embraced the development of cellulose acetate based nanocomposites in areas including plastics and packaging, membranes and separation media, water treatment and sensing. For instance, enhancing the mechanical, thermal, photocatalytic, permeability, sorption and antifouling properties of cellulose acetate based nanocomposites has extended its effective use in dechlorination and removal of heavy metals, dyes and other organic compounds.[38-47]

In this project, CA/CuO nanocomposites were prepared by a simple blending method and were used to investigate their selectivity toward metal ion uptake. Considering that CuO nanomaterials have good electrical conductivity,[48] high stability and high catalytic activity,[49] the CA/CuO nanocomposite was developed and studied with regard to its sensing performance toward Pb (II) ion detection and extraction.

EXPERIMENTAL
Reagents and materials
All chemicals and reagents were purchased from Sigma Aldrich and used directly without further treatments. Deionized water was used throughout the experiment.

Synthesis of nanomaterials
CuO nanomaterials were synthesized from a 0.1 M aqueous solution of its precursor – copper nitrate hexahydrate ($Cu(NO_3)_2.6H_2O$) and 5 wt% of carbon black (CB). Carbon black (5 wt%) was dispersed in the aqueous solution of (0.1 M) $Cu(NO_3)_2.6H_2O$ and an adequate amount of (0.5 M) sodium hydroxide (NaOH) was added dropwise to the mixture with constant stirring until the pH of the solution rose above 10. The stirring process was maintained for 12 h at 80 °C, and then the product was allowed to cool down to room temperature. The obtained CuO precipitation was washed several times with deionized water to remove any impurities.[48]

Synthesis of nanocomposite
In this study, different compositions of cellulose acetate/copper (II) oxide (CA/CuO) nanocomposite films, with CA/CuO weight ratios of 100/0, 100/1, 100/3, 100/5 and 100/10, were prepared by the blending method. These NCs were named as CA, CA/CuO (1%), CA/CuO (3%), CA/CuO (5%) and CA/CuO (10%). 1 g of cellulose acetate was dissolved in an adequate amount of acetone under magnetic stirring at ambient temperature. For each series, the required amount of CuO nanomaterials was dispersed separately in 10 mL of ethanol and magnetically stirred at 40 °C for 1 h in order to prevent coagulation and precipitation. The dispersed solution of MO/ethanol was then added dropwise to the CA/acetone solution and continuous stirring was performed for 5 h at 60 °C. Later on, the suspension was poured on a Petri dish and left to dry at room temperature. After drying, the film was removed and stored in a plastic bag until further studies.

Characterization
The CuO nanomaterial and NCs were structurally characterized by the following techniques. X-ray diffraction patterns (XRD) were taken with a computer controlled X'Pert Explorer PANalytical diffractometer. FT-IR spectra were recorded in the range from 400 to 4000 cm^{-1} on a PerkinElmer (spectrum 100) FT-IR spectrometer. The thermal behavior of the prepared nanocomposites was analyzed by a Thermo Scientific TGA in nitrogen atmosphere, at a heating rate of 10 °C/min from 23 to 1000 °C. Millipore-Q water purification was employed to produce deionized water of 18.2 MΩ.cm at 25 °C, TOC < 5 ppb. The I–V technique was employed for metal ion detection by using a Kethley Electrometer (Kethley 2400, Electrometer, USA). ICP-OES measurements were acquired by the use of a PerkinElmer ICP-OES model (Optima 7000 DV, USA). The ICP-OES instrument was optimized daily before measurement and ran as recommended by the manufacturers.

Fabrication of chemical sensor and selective detection of lead ions
The CA/CuO nanocomposite was used as a thin film for coating the surface of a silver electrode, using nafion as a binder and dried at 60.0 °C for 12 hours. The sensing ability of the composite modified AgE was evaluated using different metal ions. A two-electrode system was used for sensing metal ions, *i.e.* Ag/AgCl as a reference electrode and the composite modified AgE (with internal surface area of 0.021 cm^2)

as a working electrode. The current response was measured from 0 to 1.0 volts. The amount of acetate buffer solution was kept constant at 20.0 mL for all the measurements.

Metal ion uptake experiment

For studying the selectivity of the NC phase toward metal ions, standard solutions of 30 mg L^{-1} of each Zn^{2+}, Ni^{2+}, Pb^{2+}, Mn^{2+}, Sr^{3+}, Al^{3+}, Fe^{3+} and Ce^{3+} ions were prepared in 0.01 M potassium nitrate diluted in distilled deionized water. 35 mL of each standard solution was individually mixed with 5.2 mg of CA/CuO (5% w/w) nanocomposite. All the mixtures were mechanically shaken for 24 h at 25 °C. After 24 h of equilibration, the suspensions were filtered using Whatman 42 filter paper, and the filtrate was analyzed for the concentration of metal ions using inductively coupled plasma optical emission spectrometry (ICP-OES).[50,51] The distribution coefficient (K_d) values were determined by using Equation 1:

$$K_d = \left(\frac{C_o - C_e}{C_e} \right) \cdot \left(\frac{V}{m} \right)$$

(1)

where C_o and C_e are the initial and final concentrations before and after filtration with the nanocomposite, respectively, V refers to the volume (mL) and m is the weight of CA and nanocomposite (g).[50]

The metal ions that obtained the highest K_d values for each system were further investigated in the same batch process, with different nanocomposite fractures.

RESULTS AND DISCUSSION
Physiochemical characterization of CA/CuO nanocomposites

The chemical structure and crystallinity of CuO and CA/CuO nanocomposites were examined by typical powder X-ray diffraction and the graph is depicted in Figure 1. The general feature of the XRD patterns of the CuO nanomaterial exhibits the occurrence of only strong and sharp diffraction peaks at 2θ of 32.6, 35.5, 38.8, 48.8, 53.4, 58.3, 61.6, 66.3, 68.1, 72.4 and 75.1 Å, which could be assigned to the (110), (002), (111), (202), (020), (202), (113), (311), (220), (221) and (-222) planes of the monoclinic CuO structure with space group C2/c., respectively.[52,53] The absence of halos and other impure diffraction peaks within the detection limit of the X-ray diffraction confirms the phase purity and the presence of a highly crystalline structure of the synthesized CuO nanomaterial.

The X-ray diffraction pattern (XRD) of the CA/CuO nanocomposites shows the presence of a characteristic broad halo peak in the range of 15-30 Å, coming from the amorphous nature of CA, in addition to several sharp crystalline peaks at 35.7, 39.1, 49.0, 58.8, 61.6, 66.4, 68.1, 72.6 and 75.2 Å, which represent the presence of the CuO nanomaterial in the nanocomposite. The CuO crystalline peaks show a gradual increase in intensity with the increase in CuO concentration. The alteration in the strength of the peaks intensity of some of the phases from that observed in the nanomaterials may be caused by the strong interaction between CuO and CA. Thus, the data obtained from XRD patterns suggest the successful formation of nanocomposites from the two phases, cellulose acetate and different concentrations of CuO nanomaterials.[48]
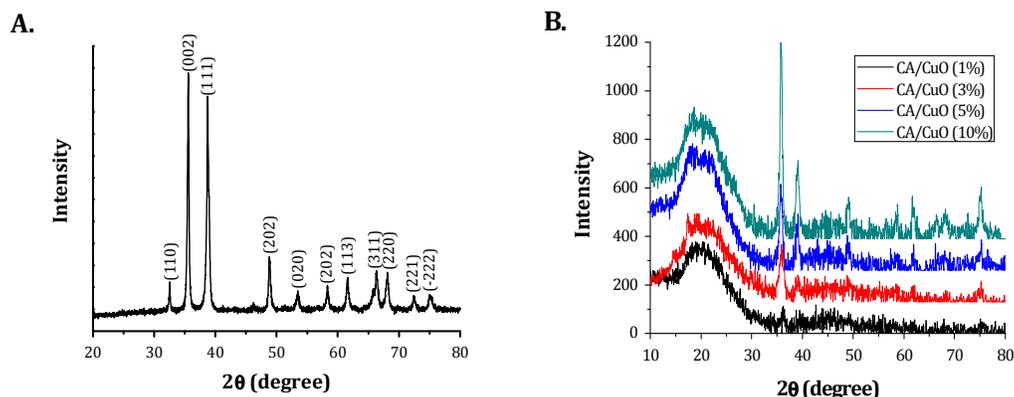

Figure 1: X-ray diffraction (XRD) patterns of (A) polymer composite of CuO and CA/CuO nanocomposite, (B) CA loaded with different percentage of CuO
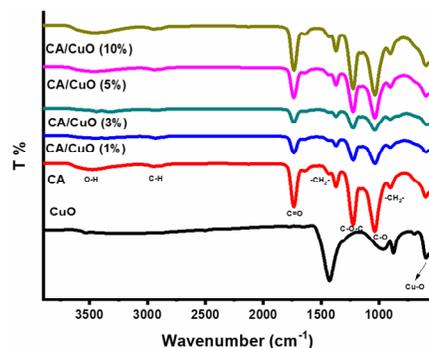
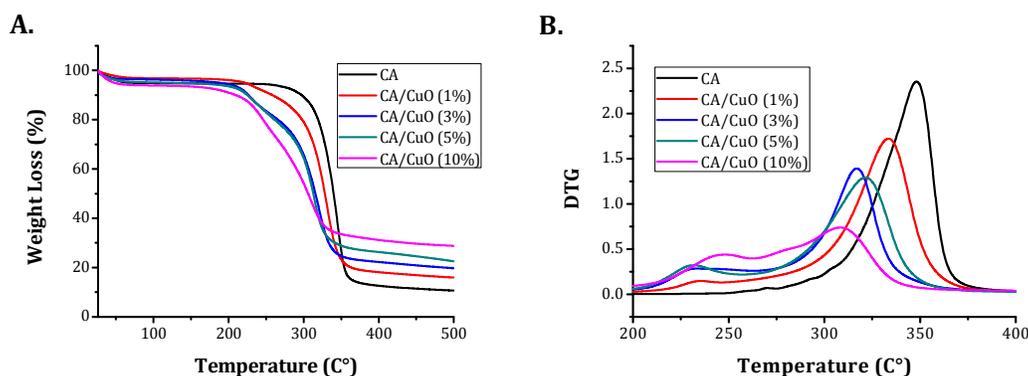Figure 2: Typical FT-IR spectra of CA, CuO and CA/CuO NCs

Figure 3: A) TGA curves of pure CA and CA/CuO NCs, B) DTA curves of pure CA and CA/CuO NCs

For studying the chemical structure and composition of the nanocomposites, the FT-IR spectra of CA, CuO and different compositions of CA/CuO nanocomposites were recorded and presented in Figure 2. As mentioned earlier, the FT-IR spectrum of CA demonstrated absorption bands at 3470, 2800-2900, 1750, 1437, 1380, 1233, 1047 and 900 cm^{-1}, which correspond to O-H, C-H, C=O, -CH$_2$-, C-O-C and C-O stretching vibration. CuO nanomaterials revealed bands at 400-600, 1430 and 3533 cm^{-1}, which are also depicted in Figure 2. The characteristic absorption bands at 500-600 cm^{-1} are responsible for the metal oxide (Cu-O) stretching vibration. The absorption bands at 3533 and 1430 cm^{-1} are assigned to the stretching and bending vibrational modes of absorbed water from surroundings.[48] The peaks of CA and CuO nanomaterials were present in the spectra of each nanocomposite, indicating the formation of NCs.[21-24]

The thermal stability of the CA/CuO nanocomposites was evaluated by thermogravimetric analysis (TGA) and differential thermal analysis (DTA). The presence of CuO nanomaterials within CA films reduces the thermal stability of CA by the addition of CuO, from 348 °C for CA to 334~308 °C for

NCs, without changing the thermal degradation behavior of the CA films. The TGA and DTA curves exhibit similar trends to that of pure CA:[54-57] dehydration, fragmentation, and finally carbonization, regardless of the CuO content (Fig. 3).

Metal ion detection and extraction
Lead ion detection

The CA/CuO nanocomposite was utilized for the selective detection of Pb^{+2} in aqueous media in order to study its chemical sensing properties toward this metal ion. The CA/CuO coated silver electrode was used as a working electrode for the detection of Pb^{+2}. The fabricated working electrode was used to measure the electrical response toward the detection of Pb^{+2}, which is shown in Figure 4.

The I-V curves for the silver electrode without coating (without CA/CuO) and after coating (with CA/CuO) were measured and shown in Figure 5. The composite coated silver electrode illustrates high current response, in contrast to the naked silver electrode, which is attributed to its metal ion sensing property originating from the NC.

Figure 5 also illustrates the electrical response of the working electrode without metal ion and

with 10.0 µL of Pb^{+2} ion in 20 mL of buffer solution (pH = 6.0). It is observed from Figure 5 that by adding the target chemical, the working electrode demonstrates a noteworthy enhancement in electrical current, which reveals the sensitivity of the working electrode toward Pb^{+2}. Consequently, by injection of the lead ion, the augmentation in the electrical response shows that the working electrode exhibits a fast and sensitive response to the target metal ion, which might be due to strong binding of the lead ion to the nanocomposite.

The influence of lead ion concentration on the electrical reaction of the working electrode was examined by the subsequent addition of lead ion into 20 mL of buffer solution (pH = 6.0). An enhancement of the electrical current with the increase in the lead ion concentration is observed, which indicates that the sensing working electrode was enhanced by the increase in the concentration of the target chemical.

The calibration curve (Fig. 6) was plotted for different concentrations of the target ion. The calibration curve portrays two sensitivity areas; the region at inferior concentrations (physisorption process) is linear up to 100 µM, with the correlation coefficient R^2 = 0.972. The sensitivity is determined from the slope of the lower concentration section of the calibration curve, which is 213.43 $\mu A.cm^{-2}.mM^{-1}$. These results were compared with others reported in the literature, as shown in Table 1.[58-60] The linear dynamic range is revealed from 10.0 µM to 100 µM, and the detection limit was estimated, based on the signal to noise ratio (S/N), to be 0.758±1.82 mM. Above 100 µM concentration, the sensor became saturated, due to chemisorption, which could be caused by the lack of free composite sites for further lead ion adsorption.[61]
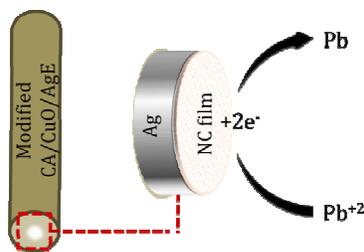

Figure 4: Fabrication of CA/CuO nanocomposite on silver electrode and illustration of the electrocatalytic reduction mechanism of lead ion on the composite modified electrode
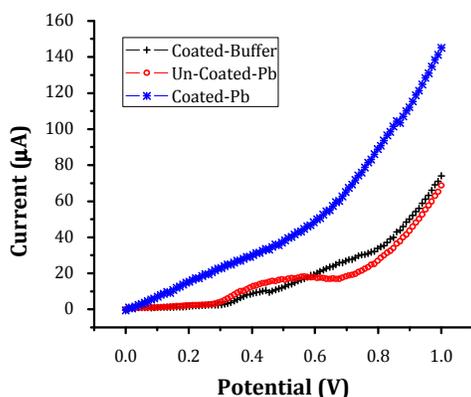

Figure 5: I–V characterization of CA/CuO NC for uncoated (in the presence of 10 mL Pb^{+2}) and coated (in the absence and presence of 10 mL Pb^{+2}) AgE
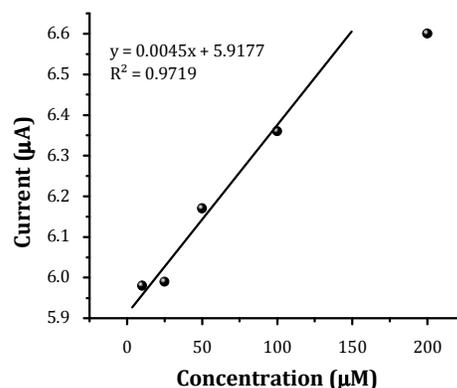
Figure 6: Calibration plot obtained from I-V characterization of CA/CuO/AgE with successive addition of lead ions

Table 1

Comparison of the detection limit of CA/CuO NCs with that of other materials employed electrochemically in Pb^{2+} detection

Material	Technique	Sensitivity	Reference
Sb_2O_3/MWCNTs	LSASV	2.694 µALµg^{-1}	58
P(Py☐co☐OT)/CF NCs	I–V	22.39 µAµM^{-1}cm^{-2}	59
GO/MA NCs	I–V	20.56 µAmM^{-1}cm^{-2}	60
CA/CuO NCs	I–V	213.43 µA.cm^{-2}.mM^{-1}	This study

Sb_2O_3/MWCNTs: Multiwall carbon nanotube modified by antimony oxide; P(Py-co-OT)/CF NCs: Poly(pyrrole-co-*o*-toluidine) copolymer and cobalt ferrite; GO/MA NCs: Graphene oxide/methylaniline nanocomposites; LSASV: Square-wave anodic stripping voltammetry
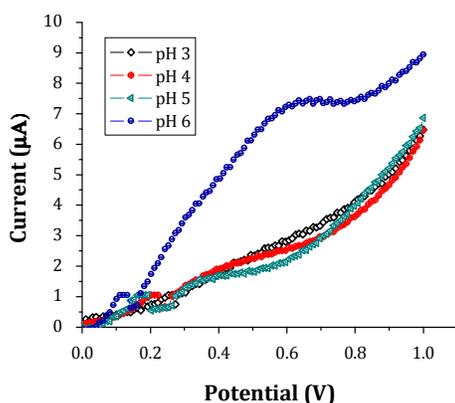

Figure 7: Current response obtained at different pH on I-Vs of CA/CuO/AgE for Pb^{+2} ions

Figure 8: Current response obtained on I-Vs of CA/CuO/AgE for different metal ions

Influence of pH

The performance of the sensor was optimized by using different pH levels (Fig. 7). The presence of the proton H$^+$ in the solution plays a crucial part in redox reactions and exerts a significant impact on electrochemical reactions. Therefore, the effect of pH on the electrochemical reaction was studied by varying the pH of the solution. It is observed from the figure that the reduction peak current increased with increasing pH value until it reached the maximum of 6.0. Hence, pH 6.0 was kept as an optimum condition for further analysis. This indicates that the electrical current of the sensor is dependent on the pH value.[62]

Selectivity of the lead ion sensor

The selectivity was investigated by using different metal ions as interfering species. Figure 8 shows the electrical response of the sensor toward different metal ions in buffer solution (pH = 6.0). The electrical response of the sensor is much higher, compared to that to other interfering metal ions, which suggests that the other metal ions have a negligible effect on the lead ion
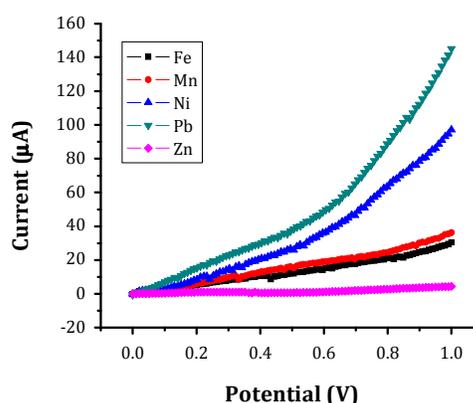
sensing property of the designed sensor, as it is more selective toward the lead ion.

The same composite material was further applied for the selective extraction of lead ions, which is explained in the following section.

Selective extraction of lead ion using nanocomposites

Selectivity studies of CA and CA/CuO nanocomposites toward different metal ions, including Zn^{2+}, Pb^{2+}, Mn^{2+}, Sr^{3+}, Al^{3+}, Fe^{3+}, Ni^{2+} and Ce^{3+}, were performed by determining the distribution coefficient (K_d) values of all the phases at the optimum pH value (pH 6.0) by Equation 1.

The distribution coefficient values of all the metal ions investigated in this study are reported in Figure 9. It can be clearly noticed from the figure that the highest distribution coefficient value was obtained for Pb^{2+} ions. The selectivity studies revealed that the CA/CuO nanocomposites were most selective towards Pb^{2+} among all the metal ions included in this study. Thus, the results imply that the CA/CuO nanocomposites are able to selectively adsorb and bind Pb^{2+} by either

electrostatic attraction or the chelating mechanism.[51]

For assessing the uptake capacity, CA and the CA/CuO nanocomposites were examined under identical conditions of pH, environment and concentration of Pb^{2+}. The nanocomposite having 3 wt% of CuO exhibited the highest uptake capacity for Pb^{2+}, with the highest distribution coefficient of 344170 mL.g^{-1} (Fig. 9), which was comparable other literature data, as shown in Table 2.[63-65] The uptake capacities of Pb^{2+} for lower and higher concentrations of CuO were not comparably significant. The decrease in the

uptake capacity for lower concentration of CuO might be attributed to being too low to be effective or to synthetic defects, whereas the decrease in the uptake capacity of the NC with further addition of CuO might be explained by a reduction of the active surface area of CuO, resulting from the aggregation of the nanomaterials in the CA matrix. These results also suggest that 3% w/w CuO is well dispersed in CA/CuO, but further increase in wt% causes a gradual decrease in dispersion and an increase in aggregation.
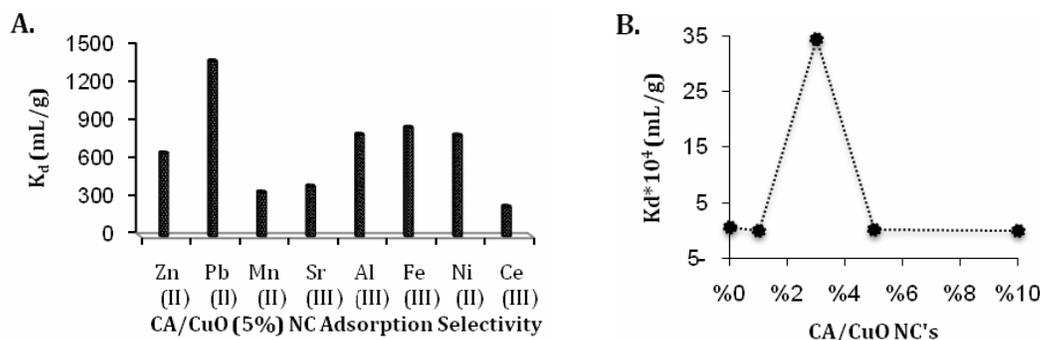

Figure 9: A) Selectivity and Pb^{2+} uptake capacity of CA/CuO NCs (3%) among different metal ions, B) Adsorption capacity of CA/CuO (3% w/w), displaying the highest uptake aptitude for Pb^{2+} with the highest K_d of 344170 mL.g^{-1}

Table 2
Comparison of uptake capacity and distribution coefficient for Pb^{2+} adsorption by CA/CuO NCs and other reported materials

Material	K_d (mLg^{-1})	Reference
Ca-doped ZnO nanoparticles	5.67×10^5	63
CdO codoped Fe_2O_3 nanofiber	1.21×10^5	64
Ni-ZnO nanoparticles	5.98×10^5	65
CA/CuO NCs	344170	This study

The possible mechanism for adsorption of Pb^{2+} might be due to strong attraction of Pb^{2+} to CA/CuO, which has a large specific surface area, and its surface is covered with OH, Cu–O– and –O–, which could be easily charged and combined with Pb^{2+}. CuO and other metal oxides have been reported as adsorbents, however, in powder form, these adsorbents are difficult to separate from the solution. To find a simple and inexpensive method for separating adsorbents from the solution, the nanocomposite of CuO and CA matrix is a convenient choice. CA/CuO has a large specific surface area, and due to the OH, Cu–O– and –O– on its surface, can easily absorb heavy metal ions. The higher Pb^{2+} concentration resulted in stronger competition among different

heavy metal ions, which might be due to a replacement of other metal ions adsorbed on the surface of the CA/CuO by Pb^{2+} and therefore, Pb^{2+} was more competitive than other metal ions. These different properties of heavy metal ions, such as ionic potential, electronegativity, easy hydroxylation and position in the Irving–Williams series, also made a difference in the removal efficiency of heavy metal ions. The preference of the sorbent for Pb^{2+} may be because the metal ions have the largest atomic weight and are paramagnetic, and the most electronegative ion has the highest standard reduction potential, as compared to other metal ions. Another reason may be related to the hydration energy and the hydrated ionic radius of heavy metals, and a lower

hydration energy was easier for the adsorption.[66] Schematically, the adsorption of Pb^{2+} onto
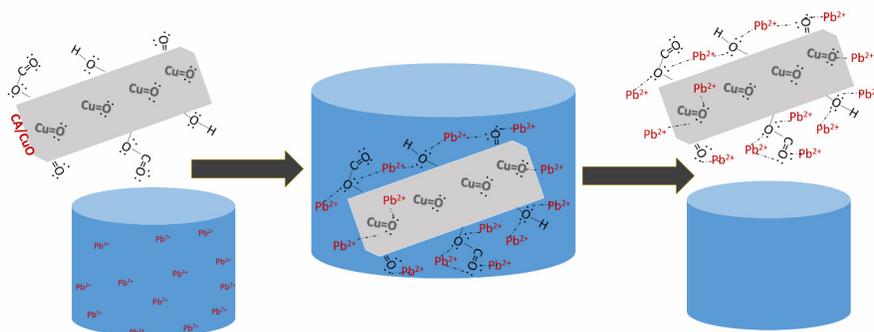
CA/CuO is shown in Figure 10.

Figure 10: Schematic diagram of Pb^{2+} adsorption by CA/CuO NCs

CONCLUSION

The synthesized CA/CuO nanocomposites were studied in terms of their sensing performance and selectivity toward metal ions. The modified AgE showed good electrical response toward lead ions detection, with linearity ($R^2 = 0.972$) up to 100 µM. The linear range exhibited a sensitivity of 213.43 µA.cm^{-2}.mM^{-1} and LOD of 0.758±1.82 mM. The electrical performance showed an optimum response at pH 6 and good selectivity toward lead ions, regardless of the interference of other metal ions. This was confirmed by the selectivity data. CA/CuO (3% w/w) displayed the highest uptake capacity for Pb^{2+}, with the highest K_d of 344170 mL.g^{-1}. Additional studies performed by ICP-OES confirmed the selectivity of CA/CuO toward Pb^{2+}, while CA/CuO (3% w/w) showed the highest uptake capacity.

REFERENCES

[1] X. M. Miao, L. S. Ling and X. T. Shuai, *Anal. Biochem.*, **421**, 582 (2012), https://doi.org/10.1016/j.ab.2011.11.031

[2] X. Yang, J. Xu, X. Tang, H. Liu and D. Tian, *Chem. Commun.*, **46**, 3107 (2010), https://doi.org/10.1039/C002137G

[3] S. Zhan, Y. Wu, Y. Luo, L. Liu, L. He *et al.*, *Anal. Biochem.*, **462**, 19 (2014), https://doi.org/10.1016/j.ab.2014.01.010

[4] L. Pujol, D. Evrard, K. Groenen-Serrano, M. Freyssinier, A. Ruffien-Ciszak *et al.*, *Front. Chem.*, **2**, 1 (2014), https://doi.org/10.3389/fchem.2014.00019

[5] E. R. E. Mojica, A. B. Tocino, J. R. L. Micor and C. C. Deocaris, *Philipp. J. Sci.*, **134**, 51 (2005), http://philjournalsci.dost.gov.ph/images/pdf/pjs_pdf/vol134no1/PDFs/a_feather_trode_sensor_for_detecting_lead_ions.pdf

[6] T. Agusa, T. Kunito, K. Ramu, C. Chamnan, P. T. K. Trang *et al.*, *Biol. Trace Elem. Res.*, **17**, 413 (2006), https://doi.org/10.11299/brte.17.413

[7] S. Z. Mohammadi, D. Afzali and D. Pourtalebi, *Cent. Eur. J. Chem.*, **8**, 662 (2010), https://doi.org/10.2478/s11532-010-0029-8

[8] G. R. de Castro, I. L. de Alcântara, P. dos Santos Roldan, D. de Fatima Bozano, P. de M. Padilha *et al.*, *Mater. Res.*, **7**, 329 (2004), https://doi.org/10.1590/S1516-14392004000200018

[9] H. P. Mhaske, V. V. Vaidya, S. Shailajan, G. Singh and K. M. Dalvi, *Nat. Environ. Pollut. Tech.*, **5**, 389 (2006), https://scholar.google.com/scholar?hl=en&as_sdt=0,5&cluster=2699688812679850959

[10] Y. Xu, J. Zhou, G. Wang, J. Zhou and G. Tao, *Anal. Chim. Acta*, **584**, 204 (2007), https://doi.org/10.1016/j.aca.2006.11.014

[11] M. Kaneko and D. Wöhrle, in "Electronic Applications", Springer, Berlin, 1988, pp. 141-228, https://doi.org/10.1007/BFb0025906

[12] J. Wang and P. Tuzhi, *Anal. Chem.*, **58**, 3257 (1986), https://doi.org/10.1021/ac00127a076

[13] A. Maines, A. Cambiaso, L. Delfino, G. Verreschi, I. Christie *et al.*, *Anal. Commun.*, **33**, 27 (1996), https://doi.org/10.1039/AC9963300027

[14] D. W. M. Arrigan, *Analyst*, **119**, 1953 (1994), https://doi.org/10.1039/AN9941901953

[15] X. Li, J. Liu, X. Ji, J. Jiang, R. Ding *et al.*, *Sensor. Actuat. B-Chem.*, **147**, 241 (2010), https://doi.org/10.1016/j.snb.2010.03.018

16 F. Meng, W. Shi, Y. Sun, X. Zhu, G. Wu *et al.*, *Biosens. Bioelectron.*, **42**, 141 (2013), https://doi.org/10.1016/j.bios.2012.10.051

17 S. A. Khayyat, S. G. Ansari and A. Umar, *J. Nanosci. Nanotechnol.*, **14**, 3569 (2014), https://doi.org/10.1166/jnn.2014.7918

18 S. Park, H. Boo and T. D. Chung, *Anal. Chim. Acta*, **556**, 46 (2006), https://doi.org/10.1016/j.aca.2005.05.080

19 S. B. Khan, S. A. Khan, H. M. Marwani, E. M. Bakhsh, Y. Anwar *et al.*, *RSC Adv.*, **6**, 110077 (2016), https://doi.org/10.1039/C6RA21626A

20 K. Akhtar, H. M. Marwani, J. Seo, E. M. Bakhsh, D. Kim *et al.*, *Polym. Compos.*, **38**, 2106 (2017), https://doi.org/10.1002/pc.23785

21 E. Y. Danish, H. M. Marwani, M. A. Alhazmi, S. B. Khan, E. M. Bakhsh *et al.*, *Bull. Mater. Sci.*, **41**, 47 (2018), https://doi.org/10.1007/s12034-018-1569-3

22 S. A. Khan, N. Khan, U. Irumd, A. Farooq, A. M. Asiri *et al.*, *Int. J. Biol. Macromol.*, **153**, 806 (2020), https://doi.org/10.1016/j.ijbiomac.2020.03.013

23 E. M. Bakhsh, S. A. Khan, H. M. Marwani, E. Y. Danish, A. M. Asiri *et al.*, *Int. J. Biol. Macromol.*, **107**, 668 (2018), https://doi.org/10.1016/j.ijbiomac.2017.09.034

24 H. M. Marwani, E. Y. Danish, M. A. Alhazmi, S. B. Khan, E. M. Bakhsh *et al.*, *Sep. Sci. Technol.*, **53**, 887 (2018), https://doi.org/10.1080/01496395.2017.1405982

25 F. Ali, S. B. Khan, T. Kamal, K. A. Alamry, E. M. Bakhsh *et al.*, *Carbohyd. Polym.*, **192**, 217 (2018), https://doi.org/10.1016/j.carbpol.2018.03.029

26 E. M. Bakhsh, F. Ali, S. B. Khan, H. M. Marwani, E. Y. Danish *et al.*, *Int. J. Biol. Macromol.*, **131**, 666 (2019), https://doi.org/10.1016/j.ijbiomac.2019.03.095

27 S. B. Khan, K. Akhtar, E. M. Bakhsh and A. M. Asiri, *Appl. Surf. Sci.*, **492**, 726 (2019), https://doi.org/10.1016/j.apsusc.2019.06.205

28 S. B. Khan, F. Ali and K. Akhtar, *Carbohyd. Polym.*, **207**, 650 (2019), https://doi.org/10.1016/j.carbpol.2018.12.032

29 A. M. Asiri, K. Akhtar and S. B. Khan, *Ceram. Int.*, **45**, 13340 (2019), https://doi.org/10.1016/j.ceramint.2019.04.028

30 F. El-Ashhab, L. Sheha, M. Abdalkhalek and H. A. Khalaf, *J. Assoc. Arab Univ. Basic Appl. Sci.*, **14**, 46 (2013), https://doi.org/10.1016/j.jaubas.2012.12.001

31 S. Fischer, K. Thummler, B. Volkert, K. Hettrich, I. Schmidt *et al.*, *Macromol. Symp.*, **262**, 89 (2008), https://doi.org/10.1002/masy.200850210

32 C. Varsha, S. K. Bajpai and C. Navin, *Int. Food Res. J.*, **17**, 623 (2010), Corpus ID: 199423472

33 F. J. Rodríguez, M. J. Galotto, A. Guarda and J. E. Bruna, *J. Food Eng.*, **110**, 262 (2012), https://doi.org/10.1016/j.jfoodeng.2011.05.004

34 W. K. Son, J. H. Youk and W. H. Park, *Carbohyd. Polym.*, **65**, 430 (2006), https://doi.org/10.1016/j.carbpol.2006.01.037

35 J. Cao, X. Ma, A. Yang and W. Xu, *Polym. Polym. Compos.*, **14**, 65 (2006), https://doi.org/10.1177%2F096739110601400106

36 W. Chen, Y. Su, L. Zhang, Q. Shi, J. Peng *et al.*, *J. Membr. Sci.*, **348**, 75 (2010), https://doi.org/10.1016/j.memsci.2009.10.042

37 M. Naghsh, M. Sadeghi, A. Moheb, M. P. Chenar and M. Mohagheghian, *J. Membr. Sci.*, **423-424**, 97 (2012), https://doi.org/10.1016/j.memsci.2012.07.032

38 W. G. Kim, J. S. Lee, D. G. Bucknall, W. J. Koros and S. Nair, *J. Membr. Sci.*, **441**, 129 (2013), https://doi.org/10.1016/j.memsci.2013.03.044

39 R. Abedini, S. M. Mousavi and R. Aminzadeh, *Desalination*, **277**, 40 (2011), https://doi.org/10.1016/j.desal.2011.03.089

40 A. Gholami, A. R. Moghadassi, S. M. Hosseini, S. Shabani and F. Gholami, *J. Ind. Eng. Chem.*, **20**, 1517 (2014), https://doi.org/10.1016/j.jiec.2013.07.041

41 V. K. Gupta, D. Pathania, P. Singh, B. S. Rathore and P. Chauhan, *Carbohyd. Polym.*, **95**, 434 (2013), https://doi.org/10.1016/j.carbpol.2013.02.045

42 L. Wu, M. Shamsuzzoha and S. M. C. Ritchie, *J. Nanopart. Res.*, **7**, 469 (2005), https://doi.org/10.1007/s11051-005-4271-5

43 L. Wu and S. M. C. Ritchie, *Chemosphere*, **63**, 285 (2006), https://doi.org/10.1016/j.chemosphere.2005.07.021

44 L. Wu and S. M. C. Ritchie, *Environ. Prog.*, **27**, 218 (2008), https://doi.org/10.1002/ep.10277

45 L. Wu, J. Chen, D. Du and H. Ju, *Electrochim. Acta*, **51**, 1208 (2006), https://doi.org/10.1016/j.electacta.2005.06.011

46 X. Ren, D. Chen, X. Meng, F. Tang, A. Du *et al.*, *Colloid Surface B*, **72**, 188 (2009), https://doi.org/10.1016/j.colsurfb.2009.04.003

47 E. Hendrick, M. Frey, E. Herz and U. Wiesner, *J. Eng. Fiber. Fabr.*, **5**, 21 (2010), https://doi.org/10.1177%2F155892501000500103

48 S. B. Khan, M. M. Rahman, K. Akhtar, A. M. Asiri, K. A. Alamry *et al.*, *Int. J. Electrochem. Sci.*, **7**, 10965 (2012), http://www.electrochemsci.org/list12.htm#issue7

49 S. Liu, J. Tian, L. Wang, X. Qin, Y. Zhang *et al.*, *Catal. Sci. Technol.*, **2**, 813 (2012), https://doi.org/10.1039/C2CY00453D

50 A. M. Asiri, S. B. Khan, K. A. Alamry, H. M. Marwani and M. M. Rahman, *Appl. Surf. Sci.*, **270**, 539 (2013), https://doi.org/10.1016/j.apsusc.2013.01.083

51 S. B. Khan, K. A. Alamry, H. M. Marwani, A. M. Asiri and M. M. Rahman, *Compos. Part B-Eng.*, **50**, 253 (2013), https://doi.org/10.1016/j.compositesb.2013.02.009

52 A. P. Moura, L. S. Cavalcante, J. C. Sczancoski, D. G. Stroppa, E. C. Paris *et al.*, *Adv. Powder Technol.*, **21**, 197 (2010), https://doi.org/10.1016/j.apt.2009.11.007

53 X. Wang, C. Hu, H. Liu, G. Du, X. He *et al.*, *Sensor. Actuat. B-Chem.*, **144**, 20 (2010), https://doi.org/10.1016/j.snb.2009.09.067

54 M. de C. C. Lucena, A. E. V. de Alencar, S. E. Mazzeto and S. d. A. Soares, *Polym. Degrad. Stabil.*, **80**, 149 (2003), https://doi.org/10.1016/S0141-3910(02)00396-8

55 M. Ali, M. Zafar, T. Jamil and M. T. Z. Butt, *Desalination*, **270**, 98 (2011), https://doi.org/10.1016/j.desal.2010.11.027

56 P. K. Chatterjee and C. M. Conrad, *J. Polym. Sci. Pol. Chem.*, **6**, 3217 (1968), https://doi.org/10.1002/pol.1968.150061202

57 A. A. Hanna, A. H. Basta, H. El-Saied and I. F. Abadir, *Polym. Degrad.*, **63**, 293 (1999), https://doi.org/10.1016/S0141-3910(98)00108-6

58 T. L. Hai, L. C. Hung, T. T. B. Phuong, B. T. T. Ha, B. S. Nguyen *et al.*, *Microchem. J.*, **153**, 104456 (2020), https://doi.org/10.1016/j.microc.2019.104456

59 D. F. Katowah, M. A. Hussein, M. M. Alam, M. A. Gabal, T. R. Sobahi *et al.*, *Chem. Select.*, **4**, 10609 (2019), https://doi.org/10.1002/slct.201902714

60 A. A. P. Khan, A. Khan, A. M. Asiri, M. M. Alam, M. M. Rahman *et al.*, *Int. J. Environ. Sci. Technol.*, **16**, 8461 (2019), https://doi.org/10.1007/s13762-019-02447-8

61 S. B. Khan, M. M. Rahman, K. Akhtar, A. M. Asiri and M. A. Rub, *PLoS ONE*, **9**, 85290 (2014), https://dx.doi.org/10.1371%2Fjournal.pone.0085290

62 S. B. Khan, M. M. Rahman, A. M. Asiri, S. A. B. Asif, S. A. S. Al-Qarni *et al.*, *Phys. E, Low Dimens. Syst. Nanostruct.*, **62**, 21 (2014), https://doi.org/10.1016/j.physe.2014.04.007

63 S. B. Khan, H. M. Marwani, A. M. Asiri and E. M. Bakhsh, *Desalin. Water Treat.*, **57**, 19311 (2016), https://doi.org/10.1080/19443994.2015.1109560

64 H. M. Marwani, M. U. Lodhi, S. B. Khan and A. M. Asiri, *J. Taiwan Inst. Chem. E*, **51**, 34 (2015), https://doi.org/10.1016/j.jtice.2015.01.018

65 M. M. Rahman, S. B. Khan, H. M. Marwani, A. M. Asiri, K. A. Alamry *et al.*, *J. Ind. Eng. Chem.*, **20**, 1071 (2014), https://doi.org/10.1016/j.jiec.2013.06.044

66 D. Ouyang, Y. Zhuo L. Hu, Q. Zeng, Y. Hu *et al.*, *Minerals*, **9**, 291 (2019), https://doi.org/10.3390/min9050291